Results in Physics 10 (2018) 449–457

Contents lists available at ScienceDirect

Results in Physics

journal homepage: www.elsevier.com/locate/rinp

Hydrothermal fabrication and characterization of ZnO/ZnS core-shell structures on white reflective films

Chin-Chi Cheng[a], Chia-Fu Cho[b], Jo Lun Chiu[b], Ching-Tsan Tsai[c], Hsiang Chen[b,*]

[a] Department of Energy and Refrigerating Air-Conditioning Engineering, National Taipei University of Technology, 10608 Taipei, Taiwan, ROC
[b] Department of Applied Materials and Optoelectronic Engineering, National Chi Nan University, 54561 Nantou, Taiwan, ROC
[c] Department of Public Health, China Medical University, Taichung 40402, Taiwan, ROC

ARTICLE INFO

Keywords:
White reflective film
ZnO/ZnS core-shell
Nanostructure
Hydrothermal fabrication
DC sputtering

ABSTRACT

In this study, white reflective films integrated with various ZnO/ZnS surface nanostructures were explored. Based on optical microscope (OM), field-emission scanning electron microscope (FESEM) and energy dispersive X-ray spectroscopy (EDS) results, nanostructures integrated with ZnS shell structures improve the material properties of a polyethylene terephthalate (PET) membrane. In addition, the surface contact angle measurements and XRD results show the hydrophilic and crystalline structures of these membranes are enhanced due to the addition of ZnS shell structures and an Au layer. White reflective PET films synthesized with various nanostructures have the potential to optimize the usage of the white reflective PET films.

Introduction

In recent years, flexible membranes and devices have attracted growing attention in the energy, light source [1], photo detector [2] and biomedical sensor/device industries. Several plastic materials, including polyester, polypropylene (PP), polyethylene terephthalate (PET), polystyrene (PS), rubber, Kevlar and other fibers [3,4] are some of the versatile components which utilize flexible membranes and devices. These flexible films which play an important role in improving the performance of solar cells [5], light emitting diodes (LEDs) [6], and electronic skins [7]. Among these flexible membranes, white reflective film is often used as a backlight module for improving the luminescence of sconces, Troffer Fixtures, liquid-crystal display (LCD), televisions, mobile phones [8–10], etc. Polyethylene terephthalate (PET) is one of the most frequently used materials as a white reflective film. Fig. 1 presents the chemical structure of PET.

Due to the wide and direct bandgap of ZnO and ZnS, these two compound materials have been intensively employed as optoelectronic materials to produce electronic and photonic devices, such as transductors [11], gas sensors [12], optical devices [13], field emitters, light sensors, biological applications, optical devices, LEDs, and electroluminescence devices [14]. Recently, ZnS/ZnO nanostructures have been employed as components of novel solar cells and photodetectors. Along with nanostructure improvements, core/shell structured ZnO/ZnS have been found to improve physical and chemical properties of ZnO nanostructures. There are several studies discussing the methods to control fabrication of ZnO/ZnS cores/shells and obtain different morphologies [15]. ZnS/ZnO nanostructures with appropriate ZnS deposition times have been shown as having the strongest ZnS crystalline structures [16]. The performance of the ZnO/ZnS core/shell structures has been further enhanced through the piezo-phototronic effect to create a high-performance broadband UV/visible photodetectors [17]. Detailed comparisons between this work and the previous related works are shown in Table 1.

In order to verify the optical performance of white reflective film/membranes strengthened by fabricated nanostructures, Au film, ZnO nanostructures [24] and ZnO/ZnS core-shell structures [25] were integrated on a PET membrane by DC sputtering and a low-temperature hydrothermal method. The formed multi-layer reflective membranes included a normal white PET membrane, a PET membrane with a Au layer, ZnO nanostructures on a PET membrane, ZnO nanostructures on a Au/PET membrane, ZnO/ZnS core-shell structures on a PET mem-

* Corresponding author.
E-mail address: hchen@ncnu.edu.tw (H. Chen).

https://doi.org/10.1016/j.rinp.2018.06.049
Received 30 March 2018; Received in revised form 24 June 2018; Accepted 24 June 2018
Available online 28 June 2018

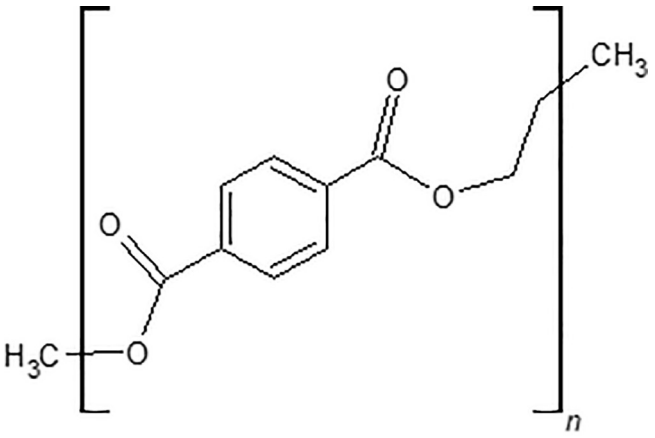

Fig. 1. Chemical structure drawing of PET.

brane. To characterize the surface structures, element compositions and crystal phases of fabricated multi-layer reflective membranes, a field-emission scanning electron microscope (FE-SEM), energy dispersive X-ray spectroscopy (EDS) and X-ray Diffraction (XRD) were utilized. Moreover, optical and hydrophobic properties were further evaluated by an optical microscope and contact angle measurement. The results indicate that ZnO/ZnS core shell structures on a PET membrane can modulate the nanostructure, enhance optical properties, and vary hydrophilicity for future applications.

Experiments

A hydrothermal method, which has advantages of low cost and simple fabrication, was used to integrate nanostructures in a room temperature environment with better control of the final product's composition. This approach is suitable for processing and manufacturing nanorods and shell structures for various applications. Fig. 2 presents the fabricating procedures of multi-layer reflective PET

Table 1
The correlated research topics in observations of SEM images and AFM images on ZnO NRs, ZnO/ZnS core-shell structures and other compositions.

	Morphologies	Main research	Apparatus
This study	Shows the roughness and inhomogeneous array that compare to the dots and strips.	ZnO/ZnS core-shell structure on white reflective film by hydrothermal method	SEM to pair up with OM
#a [18]	Displayed obviously smooth characteristics.	Thermally evaporated zinc oxide thin films on polyethylene terephthalate substrates	AFM
#b [19]	Plenty of SEM images has been displayed in many different components in this study, and one showed the ZnO nanoflowers as the same as our study because of Au particles.	Nanostructured ZnO surfaces	SEM
#c[20]	Shows better adhesion between matrix and fiber.	ZnO nanostructures on Kevlar fiber	SEM
#d[21]	Hexagonal (wurtzite-type).	Zinc oxy-sulfide/cubic-tin sulfide interface	AFM to pair up with GIXRD
#e [22]	ZnS exists as a layer of nanoparticles, and both coverage degree and sulfur content increase with the growth cycles.	ZnO/ZnS Core-Shell Nanowires-GaN Heterojunction	SEM
#f [23]	The rod diameters were increased because of the sulfurization process.	ZnO@ ZnS Core-Shell structures on ITO substrates	SEM

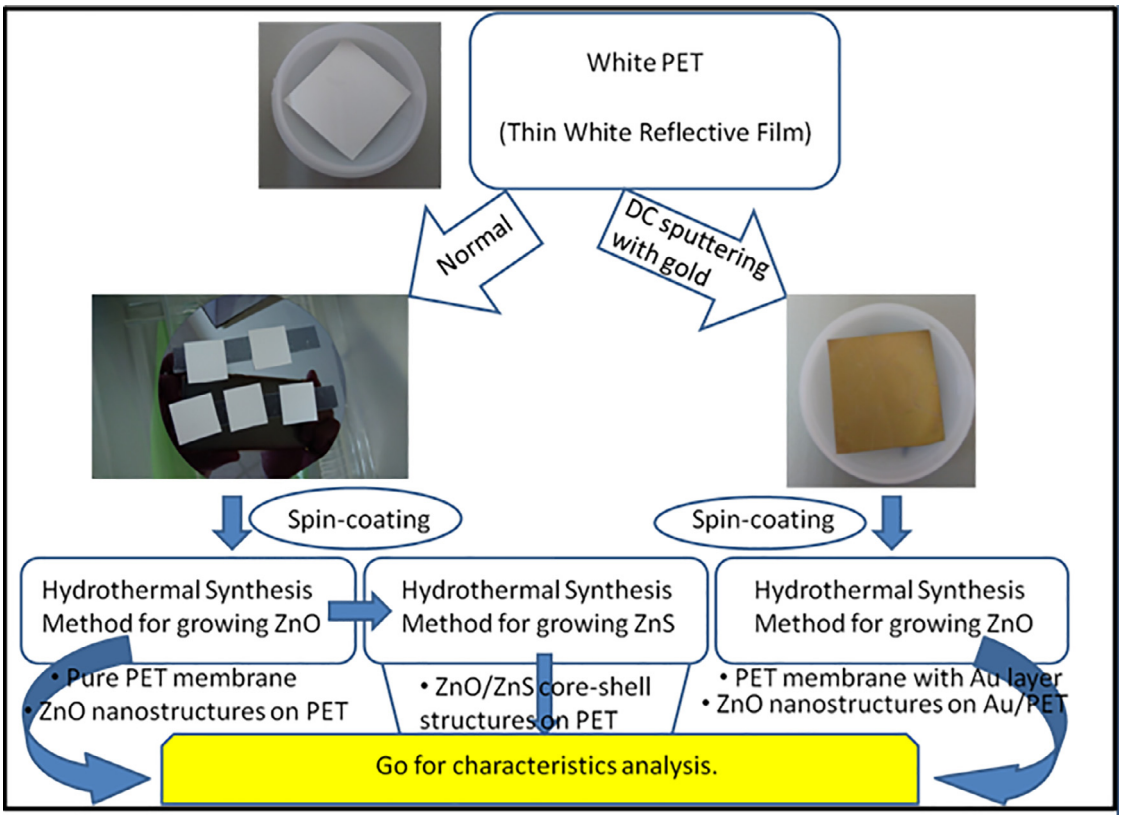

Fig. 2. Fabricating procedures of multi-layer reflective PET membranes.

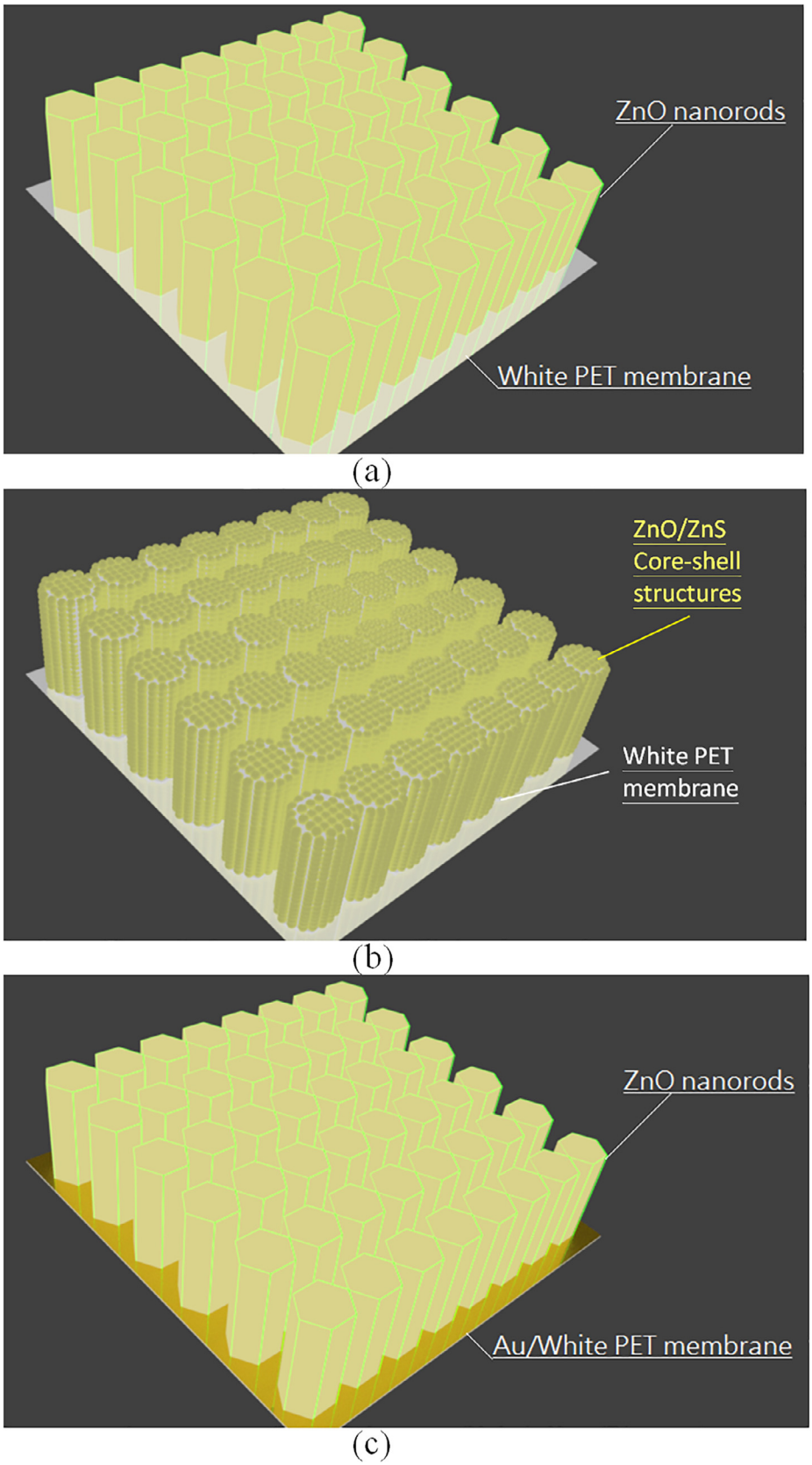

Fig. 3. Schematic pictures of (a) ZnO nanostructures on a white PET membrane, (b) ZnO/ZnS core-shell structures on a white PET membrane, (c) ZnO nanostructures on an Au/white PET membrane.

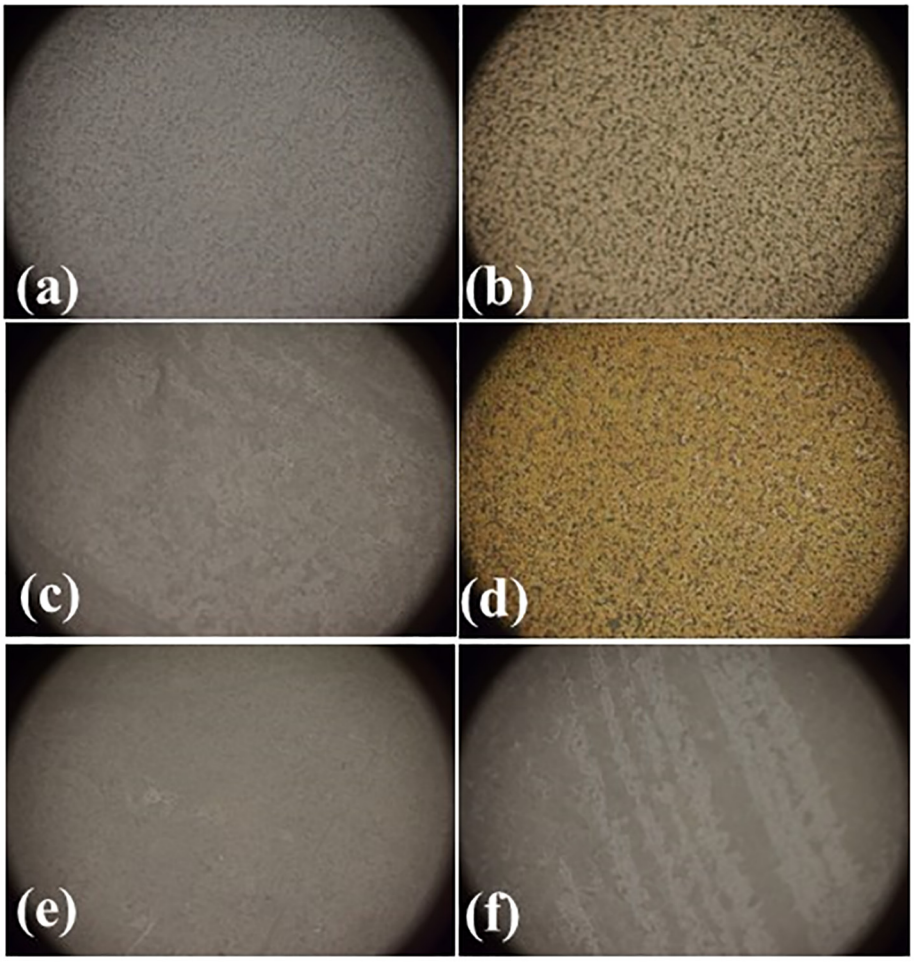

Fig. 4. Optical microscopic images of (a) a white PET membrane, (b) a PET membrane with a Au layer, (c) ZnO nanostructures on a PET membrane, (d) ZnO nanostructures on a Au/PET membrane, ZnO/ZnS core-shell structures on a PET membrane with a sulfurization period of (e) 10 and (f) 20 min.

membranes. White reflective PET membranes (QA, Eleceram Technoogy Co., Ltd., Taiwan) with a size of $2 \times 2\,cm^2$ and a thickness of 10 μm were cleansed first. Then, five types of multi-layer reflective PET membranes were prepared according to the following procedures:

(1) Normal PET membrane: The cleansed PET membrane.
(2) ZnO nanostructures on a PET membrane: The ZnO seed layer was fabricated on the cleansed PET membrane by spin coating with a lab-made solution composed of zinc acetate and ethanol. Then, ZnO nanorods were grown hydrothermally for two hours on the seeded PET membrane at 80° C in a solution containing zinc nitrate hexahydrate and hexamethylenetetramine.
(3) ZnO/ZnS core-shell structures on a PET membrane: After the cleansing and drying process, PET membranes with ZnO nanorods were placed in a solution containing sodium sulfide nonahydrate at 70° C for 10 and 20 min to synthesize the ZnO/ZnS core–shell structures.
(4) PET membrane with a Au layer: A cleansed PET membrane was synthesized with a Au layer of 5 nm in thickness by DC sputtering (ULVAC Co. Japan).
(5) ZnO nanostructures on a Au/PET membrane: A ZnO seed layer was fabricated on a Au/PET membrane by spin coating with the lab-made solution. Then, ZnO nanorods were grown hydrothermally on the seeded PET membrane for two hours at 80 °C in a solution containing zinc nitrate hexahydrate and hexamethylenetetramine.

The schematic pictures of fabricated multi-layer reflective membranes are illustrated in Fig. 3 to illustrate the nanostructures on the membrane surfaces. In Fig. 3(a), ZnO nanorods were synthesized vertically on a white PET membrane. Based on Fig. 3(a), ZnS shells were integrated on ZnO nanorods to form the ZnO/ZnS core-shell structures on a PET membrane, as shown in Fig. 3(b). Fig. 3(c) presents the ZnO nanorods fabricated on a Au/PET membrane. In order to measure the surface structures and performance of the fabricated multi-layer reflective membranes, FE-SEM, EDS, XRD, optical microscope and contact angle examinations were carried out.

Results and discussions

In order to understand the multi-layer reflective membranes affected by various nanostructures, surface morphologies measured by optical microscope (OM) are presented in Fig. 4. The optical microscopic images of the white PET membrane and the PET membrane with a sputtered Au layer are presented in Fig. 4(a) and (b). The Au layer seems to reflect the roughness of the PET membrane in Fig. 4(b). In Fig. 4(c), (e) and (f), the synthesized ZnO and ZnO/ZnS nanostructures form gray-white strips on the PET membrane and make the surface smoother, thereby increasing its reflective effect. This can also be verified from Fig. 4(d), where the ZnO nanostructures increase the brightness of the Au/PET membrane. Therefore, the integrated nanostructures improve the surface reflective performance of the PET membrane.

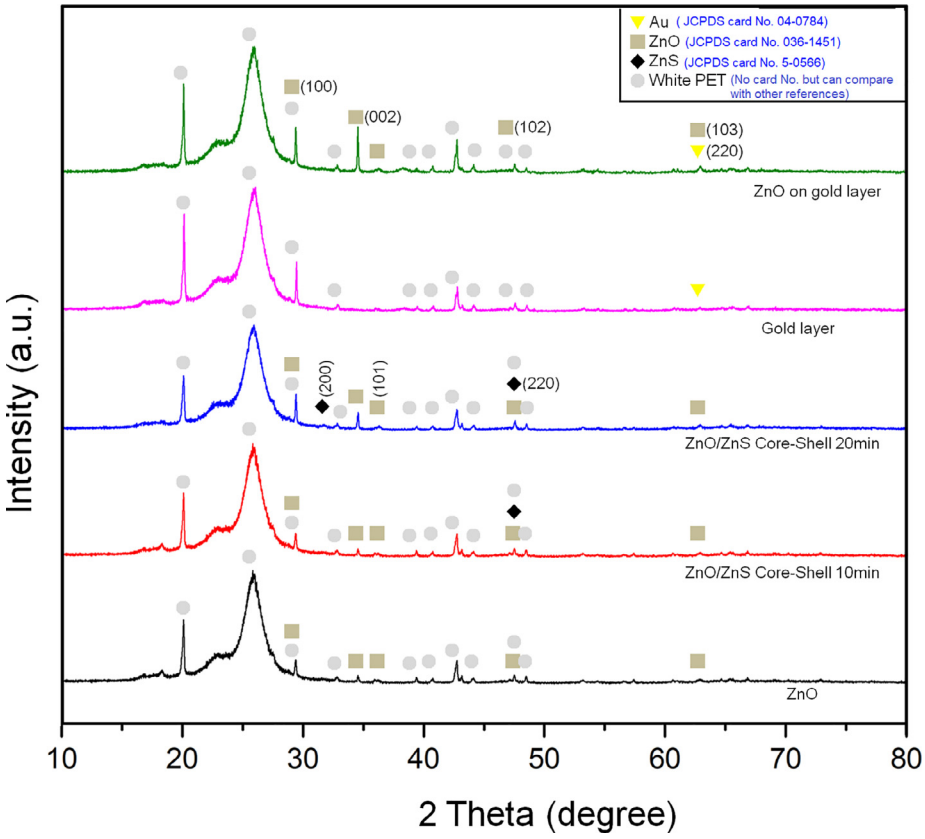

Fig. 5. From top to bottom: XRD patterns of ZnO nanostructures on a Au/PET membrane, a Au/PET membrane, ZnO/ZnS core-shell structures on a PET membrane under sulfurization periods of 10 and 20 min, ZnO nanostructures on a PET membrane.

The crystallization of multi-layer reflective membranes affected by various nanostructures was explored using XRD. From top to bottom, Fig. 5 shows XRD patterns of ZnO nanostructures on the Au/PET membrane, the Au/PET membrane, ZnO/ZnS core-shell structures on the PET membrane with sulfurization periods of 10 and 20 min, and ZnO nanostructures on the PET membrane. In Fig. 5, all the diffraction peaks are compared with the information listed in the Joint Committee on Powder Diffraction Standards (JCPDS) Table. The X-ray diffraction patterns of ZnO (JCPDS card No. 036-1451) (100), (002), (101), (102) and (103) were observed in most of the membranes, except the Au/PET membrane. The XRD pattern of Au (JCPDS card No. 04-0784) (220) is shown in the membrane with the Au layer. The XRD pattern of ZnS (JCPDS card No. 5-0566) (220) is displayed in the ZnO/ZnS core-shell structures on the PET membrane with sulfurization periods of 10 and 20 min. However, the XRD pattern of ZnS (200) only appears in the ZnO/ZnS core-shell structures on the PET membrane under a sulfurization period of 20 min. This indicates that the amount of ZnS crystals increased with the sulfurization time.

The elemental contents of the multi-layer reflective membranes affected by various nanostructures were explored using EDS. The measured results are presented in Fig. 6. In Fig. 6(a), the contents of ZnO nanostructures on the PET membrane include carbon, oxygen, sulfur and zinc with weight percentages of 31.24, 22.91, 1.13 and 44.72 percent, respectively. In Fig. 6(c) and (d), the content percentages of sulfur and zinc of ZnO/ZnS core/shell nanostructures on the PET membrane were (3.85, 42.19)/ (S, Zn) and (5.05, 65.76)/(S, Zn), respectively. These results indicate that the sulfur content increased with the sulfurization time. These results were similar to those measured by XRD in Fig. 5.

To examine the surface morphologies of the multi-layer reflective membranes which were affected by various nanostructures, a FESEM was utilized. The measured results are presented in Fig. 7. In Fig. 7(a)–(c), ZnO nanostructures on the PET membrane are clearly observed and form a rough and varied distribution. In Fig. 7(d)–(f), the ZnS shell synthesized on ZnO nanostructures are observed. However, due to less sulfurization time, the nanostructures on the PET membrane are still rough and varied. In Fig. 7(g)–(i), the dense ZnO/ZnS core/shell nanostructures are presented under sulfurization periods of 20 min. The dense ZnS shell coating improved the surface property and increased the reflectiveness of the PET membrane. In Fig. 7(j)–(l), the sputtered Au layer also benefited from the growth of ZnO nanostructures to form the smooth and well-distributed surface of the Au/PET membrane. These results were similar to those presented in Fig. 4.

The hydrophilicity of the multi-layer reflective membranes affected by various nanostructures was measured by surface contact angle testing. The measured results are shown in Fig. 8. In Fig. 8(a), (b) and (e), the surface contact angles of a PET membrane, ZnO nanostructures on a PET membrane, and the Au/PET membrane were 83.7, 63.7, and 70.6°, respectively. This indicates the hydrophobic properties of these membranes. In Fig. 8(c)–(f), the surface contact angles of ZnO/ZnS core-shell structures on a PET membrane under a sulfurization time of 10 and 20 min and ZnO nanostructures on the Au/PET membrane are 17.0, 40.6 and 23.2°, respectively. This indicates the hydrophilic properties of these membranes, due to the addition of ZnS shell structure and the Au layer.

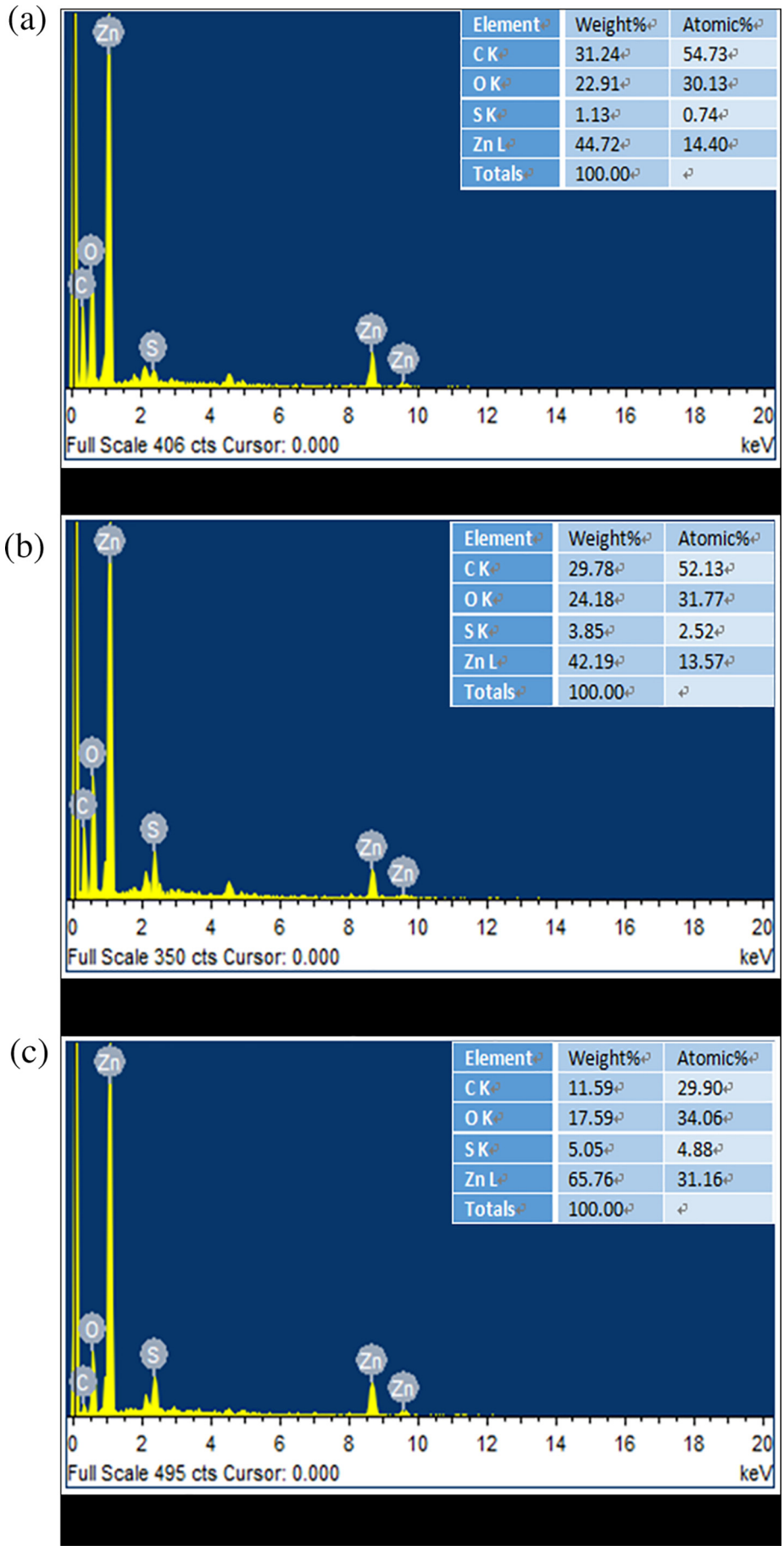

Fig. 6. EDS graphs of (a) ZnO nanostructures on a PET membrane and ZnO/ZnS core/shell nanostructures on a PET membrane under sulfurization times of (b) 10 and (c) 20 min.

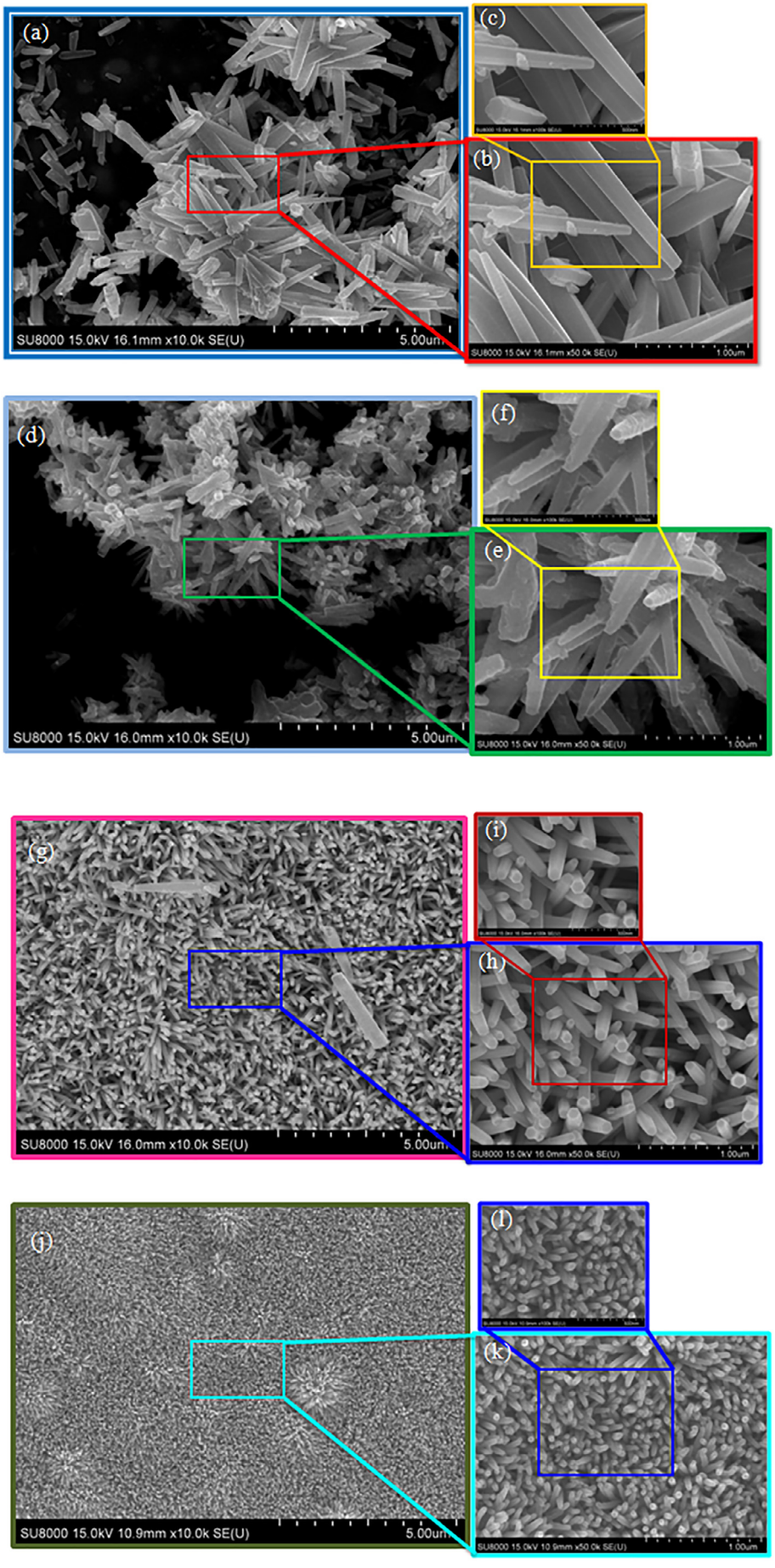

(caption on next page)

Fig. 7. FE-SEM images of (a)–(c) ZnO nanostructures on a PET membrane with different magnification rates. ZnO/ZnS core/shell nanostructures on a PET membrane under sulfurization periods of (d)–(f) 10 and (g)–(i) 20 min, (j)–(l) ZnO nanostructures on a Au/PET membrane, with magnification rates of 10 k, 50 k and 100 k, respectively.

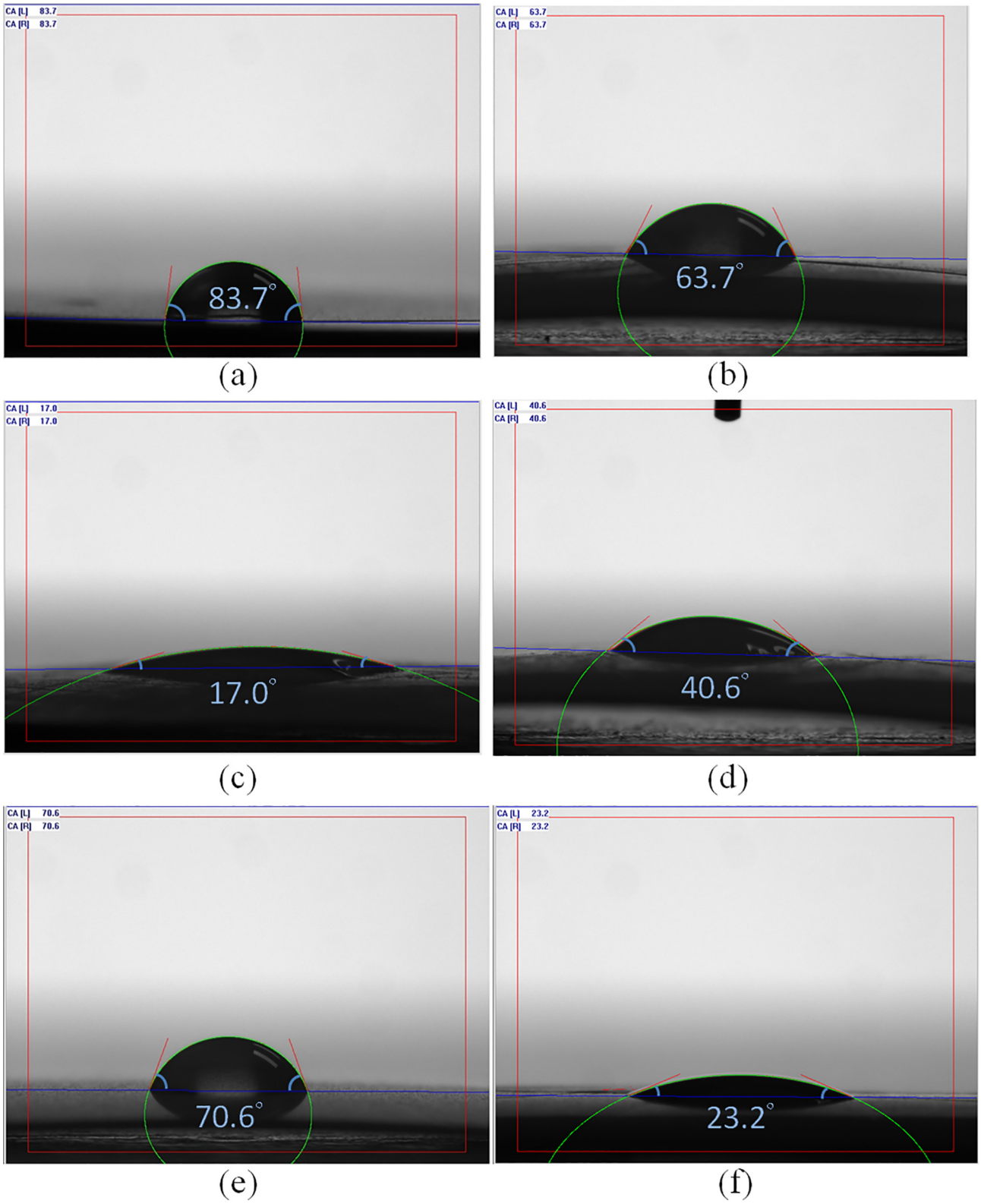

Fig. 8. Surface contact angle measurements of (a) a PET membrane, (b) ZnO nanostructures on a PET membrane, ZnO/ZnS core-shell structures on a PET membrane under sulfurization periods of (c) 10 and (d) 20 min, (e) a Au/PET membrane, (f) ZnO nanostructures on a Au/PET membrane.

Conclusions

In this research, white reflective PET membranes were coated with various nanostructures including an Au layer, ZnO nanostructures, ZnO/ZnS core-shell structures, and ZnO nanostructures. Based on OM, FE-SEM and EDS results, the ZnS shell integrated nanostructures show the possibility to improve the surface reflective performance of the PET membrane. Moreover, from the results of the surface contact angle test and XRD, the hydrophilic and crystalline properties of these membranes are enhanced by the addition of a ZnS shell structure and an Au layer. Therefore, white reflective PET films synthesized with various nanostructures are promising for future optoelectronic devices.

Acknowledgement

This study was supported by the Ministry of Science and Technology (MOST) Taiwan, Republic of China, under contract no. MOST 104-2221-E-260-002 -MY3.

References

[1] Cheng E., Medical device light source; 2017, Google Patents.
[2] Tian W, et al. Flexible ultraviolet photodetectors with broad photoresponse based on branched ZnS-ZnO heterostructure nanofilms. Adv. Mater. 2014;26(19):3088–93.
[3] Vaiano V, et al. Degradation of terephthalic acid in a photocatalytic system able to work also at high pressure. Chem Eng J 2017;312:10–9.
[4] Azpitarte I, et al. Suppressing the thermal and ultraviolet sensitivity of Kevlar by infiltration and hybridization with ZnO. Chem Mater 2017;29(23):10,068–74.
[5] Lu S, et al. Large area flexible polymer solar cells with high efficiency enabled by imprinted Ag grid and modified buffer layer. Acta Mater 2017;130:208–14.
[6] Li X, Zhang P. Flexible led light string and method of making; 2017, Google Patents.
[7] He H, et al. A flexible self-powered T-ZnO/PVDF/fabric electronic-skin with multi-functions of tactile-perception, atmosphere-detection and self-clean. Nano Energy 2017;31:37–48.
[8] Sato Y, Sakaguchi Y, Watanabe O. White reflective film; 2012, Google Patents.
[9] Sakaguchi Y, Kawata Y, Suzuki M. White reflective film for edge-light type backlight, and liquid crystal display backlight using same; 2017, Google Patents.
[10] Edmond MD, Pickard PK. Lensed troffer-style light fixture; 2018, Google Patents.
[11] Asif MH, Usman Alia SM, Nura O, Willandera M, Brännmarkb C, Strålforsb P, Englundb UH, Elinderb F, Danielssonc B. Biosens Bioelectron 2010;25:2205.
[12] Wang J, Sun XW, Yang Y, Huang H, Lee YC, Tan OK, Vayssieres L. Nanotechnology 2006;17:4995.
[13] Takanezawa K, Hirota K, Wei QS, Tajima K, Hashimoto K. J Phys Chem C 2007;111:7218.
[14] Fang X, Wu L, Hu L. Adv Mater 2011;23:585.
[15] Ghrib T, Al-Messiere MA, Al-Otaibi AL. J Nanomater 2014;2014:1.
[16] Yu T, Wang K, Chen Y, Sheu M, Chen H. Effect of deposition time on ZnO/ZnS coreshell nanostructures on silicon substrate. Chalcogenide Lett 2017;14.
[17] Rai SC, Wang K, Ding Y, Marmon JK, Bhatt M, Zhang Y, Zhou W, Wang ZL. Piezo-phototronic effect enhanced UV/visible photodetector based on fully wide band gap type-II ZnO/ZnS core/shell nanowire array. ACS Nano 2015;9:6419–27.
[18] Faraj M, Ibrahim K. Optical and structural properties of thermally evaporated zinc oxide thin films on polyethylene terephthalate substrates. Int J Polym Sci 2011;2011.
[19] Laurenti M, Stassi S, Canavese G, Cauda V. Surface engineering of nanostructured ZnO surfaces. Adv Mater Interfaces 2017;4.
[20] Majumdar A, Singh Butola B, Awasthi N, Chauhan I, Hatua P. Improving the mechanical properties of p-aramid fabrics and composites by developing ZnO nanostructures. Polym Compos 2017.
[21] Sanal K, Nair P, Nair M. Band offset in zinc oxy-sulfide/cubic-tin sulfide interface from X-ray photoelectron spectroscopy. Appl Surf Sci 2017;396:1092–7.
[22] Li R, Wei Z, Fang X, Wang Y, Li Y, Wang D, et al. Localized states dependent electroluminescence from ZnO/ZnS core-shell nanowires-GaN heterojunction. ACS Appl Nano Mater 2018.
[23] Huang W, Chen Y, Weng W, Chiu J, Li C, Tsai Y, Lin P, Lu C, Su W, Lin C. Fabrication and characterization Of ZnO@ ZnS core-shell structures on to substrates. J Ovonic Res 2018;14:63–9.
[24] Tian ZR, et al. Complex and oriented ZnO nanostructures. Nat. Mater. 2003;2(12):821.
[25] Hu Y, et al. A microwave-assisted rapid route to synthesize ZnO/ZnS core–shell nanostructures via controllable surface sulfidation of ZnO nanorods. CrystEngComm 2011;13(10):3438–43.